AIP | Applied Physics Letters

Stress distribution of GaN layer grown on micro-pillar patterned GaN templates

S. Nagarajan, O. Svensk, M. Ali, G. Naresh-Kumar, C. Trager-Cowan et al.

Citation: Appl. Phys. Lett. **103**, 012102 (2013); doi: 10.1063/1.4813077
View online: http://dx.doi.org/10.1063/1.4813077
View Table of Contents: http://apl.aip.org/resource/1/APPLAB/v103/i1
Published by the AIP Publishing LLC.

Stress distribution of GaN layer grown on micro-pillar patterned GaN templates

S. Nagarajan,[1,a)] O. Svensk,[1] M. Ali,[1] G. Naresh-Kumar,[2] C. Trager-Cowan,[2] S. Suihkonen,[1] M. Sopanen,[1] and H. Lipsanen[1]
[1]*Department of Micro and Nanosciences, Aalto University, P.O. Box 13500, FI-00076 Aalto, Finland*
[2]*Department of Physics, SUPA, University of Strathclyde, Glasgow G4 0NG, United Kingdom*

(Received 7 March 2013; accepted 18 June 2013; published online 3 July 2013)

High-resolution Raman mapping of the stress distribution in an etched GaN micro-pillar template and a 5 μm thick GaN layer grown on a micro-pillar patterned GaN template is investigated. Raman mapping of the E_2 (high) phonon shows differences in stress between the coalescing boundary, the top surface of the pillar region and around the GaN micro-pillar. Increased compressive stress is observed at the coalescing boundary of two adjacent GaN micro-pillars, when compared to the laterally grown GaN regions. The electron channeling contrast image reveals the reduction of threading dislocation density in the GaN layer grown on the micro-pillar patterned GaN template. © *2013 AIP Publishing LLC*. [http://dx.doi.org/10.1063/1.4813077]

GaN based light emitting diodes (LEDs) are widely used in general illumination, displays, and traffic lights. Even though the efficiency of GaN based LEDs has improved dramatically within the last few years, there are still many ways to improve the overall efficacy of these light sources. Internal quantum efficiency (IQE) of GaN LEDs can be improved by further improvements in the crystalline quality of the materials by reducing threading dislocation density (TDD).[1] High TDD of the GaN layers originates mainly from the large lattice mismatch between the heteroepitaxial substrate and the epilayer.[2] Lattice mismatch together with differences in thermal expansion coefficients causes biaxial stress to the epitaxial layer. GaN is compressively strained, when c-plane sapphire is used as a substrate material.[3] TDs and other defects are present in GaN and give rise to stress-relaxation due to the growth of GaN layer on sapphire substrate.[4] Formation of dislocations decreases the high compressive stress of the epitaxial GaN layer. Several methods have been employed to reduce the TDD in GaN layers grown on sapphire substrates: epitaxial lateral overgrowth (ELO),[5] pendeo-epitaxy (PE),[6] patterning of substrates,[7] etc. Among these methods, ELO has been widely studied and proven to be a powerful technique to reduce TDD by 3–4 orders of magnitude.[5] Typically, in this technique, GaN layer is overgrown laterally from the boundary of dielectric mask stripe (SiO_2), and it coalesces at the center of the stripes. However, TDs originate from the coalescence boundaries causing differences in crystalline quality and stress between the laterally overgrown and the vertically grown region in the GaN layer.[8] On the other hand, maskless PE method has been proposed to enhance the material quality. However, GaN layers grown by using this technique also exhibit spatial variations in stress.[9] In this work, we study the GaN layer grown on a micro-pillar patterned GaN template using Raman spectroscopy. In order to clearly understand the spatial variations in stress in the GaN layer grown on the micro-pillar patterned GaN template, high-resolution spatial Raman mapping is performed.

GaN structures were grown by metal organic vapor phase epitaxy (MOVPE). A 200-nm thick nickel mask was deposited onto a 3-μm thick undoped GaN buffer layer grown on a c-plane sapphire substrate. The nickel mask was patterned with circular elements using standard photolithographic techniques. Regrowth of GaN on the pillar patterned template was performed under a high V/III-ratio of 1500 in H_2 ambient at a pressure of 200 Torr. Growth parameters were optimized to achieve the high lateral growth rate needed for coalescence of the pillars. Circular pillars form hexagonal pattern during regrowth because some GaN planes grow faster than others. During regrowth, the pillars form sixfold symmetry around the c-axis with {1 −1 0 0} sidewalls. The laterally grown GaN from the side walls of the pillar makes no contact with the sapphire substrate due to the high growth temperature. This small gap between the GaN and sapphire changes into a three dimensional void at the coalescence boundary. The reason for this is the limited access of the reactant species to the close proximity of the GaN/sapphire interface, when the opening between adjacent pillars gets narrow sufficiently. As a result of regrowth, a network of embedded 3D-voids is formed around the hexagonal pillars. More detailed information of the patterning process and the regrowth of GaN on micro-pillar templates is presented elsewhere.[10,11] Raman scattering experiments were performed on the top surface of the GaN micro-pillar template before regrowth and on a 5 μm thick completely coalesced GaN layer grown on the micro-pillar patterned template. The spectra were acquired at room temperature in a confocal Raman backscattering geometry using the 532 nm line from a frequency-doubled Nd:YAG laser for excitation. The laser light was coupled into the microscope using a single-mode fiber and brought onto a sample using a dichroic mirror and a 100× microscope objective (NA 0.9). The laser beam diameter is about 400 nm with the spectral resolution of 0.02 cm^{-1}. In the detection beam path, Rayleigh-scattered light was filtered out using an edge filter and a 50 μm core-

[a)]E-mail: nagarajan.subramaniyam@aalto.fi

diameter fiber was used as a confocal pinhole, providing the spatial resolution of about 300 nm. The backscattered light was then directed to an ultra-high throughput spectrometer equipped with 1800 g/mm grating and thermoelectrically cooled electron-multiplication charge-coupled device detector. The XY positioning of the sample was achieved using a piezoelectric scanning stage, and stepper motor was used for focus control. The scanning area was 15 μm × 8 μm. The scanning area is divided into 80 lines, and each line has 200 measurement points. First, the Raman mapping of the E_2 (high) phonon was measured in the range of 560 cm^{-1} to 580 cm^{-1}. In order to obtain the precise E_2 (high) phonon frequency position, the measured values were fitted with a Lorentzian line shape. Second, the A_1(LO) phonon mapping was performed in the range of 730 cm^{-1} to 760 cm^{-1}. The A_1(LO) phonon frequency position was fitted using Gaussian lineshape.

The inset of Figure 1 shows a cross-sectional scanning electron microscope (SEM) image of the patterned GaN micro-pillar template prior to regrowth. The height and width of the pillars are 3 μm and 2 μm, respectively. Figure 1 also shows the Raman spectra of GaN micro-pillar measured at the center and edge of the pillar top. The Raman spectra reveal a sharp E_2 (high) phonon mode at 567.7 cm^{-1} at the center of the micro-pillar. The position of the nonpolar E_2 (high) phonon mode is a sensitive indicator for strain.[12] The E_2 (high) phonon frequency is in agreement with the thick, strain-free GaN layer of 567.6 cm^{-1}, which indicates that the GaN micro-pillar is almost stress-free.[13] A large proportion of the surface area of a GaN pillar is surrounded by free space which affects the stress inside the crystal. The A_1 (LO) phonon mode is observed at 734.6 cm^{-1} in the center of the micro-pillar and is shifted to 739.3 cm^{-1} at the edge. In addition, the weak features related to forbidden E_1(TO) and A_1(TO) phonons are observed at 559.0 cm^{-1} and 534.1 cm^{-1} at the edge of the micro-pillars. The observed A_l(LO) phonon frequency shift at the edge to higher frequencies compared to the center of the micro-pillar has been explained previously by (i) LO phonon-plasmon coupling due to Si-doping[8] and (ii) mixing of the A_1(LO) with the E_1(LO) phonon.[14] We rule out the possibility of LO phonon-plasmon coupling in our case due to the undoped nature of the GaN micro-pillar template. This A_1(LO) frequency shift at the edge of the pillar is therefore related to the mix of A_1(LO) and E_1(LO) phonon frequencies for intermediate phonon propagation directions between the c and a axes. This will be discussed later in the text. Also, the E_1(TO) and A_1(TO) phonon modes are observed from the edge due to off-axis phonon propagation, which also supports the A_1(LO) phonon shift to higher frequencies.[15]

In order to understand the strain distribution in the overgrown GaN layer, we have performed Raman mapping from 560 to 580 cm^{-1} to cover the E_2 (high) phonon frequency. Figure 2(a) shows an optical microscope image of the top surface of a smooth 5-μm-thick-fully coalesced GaN layer grown on a GaN micro-pillar template. The hexagonal GaN pattern with the coalescing boundary between two micro-pillars and the coalescing point between three GaN micro-pillars can be seen as brighter areas in the image. The cross-sectional SEM image of the void structure is shown in Ref. 11. Figure 2(b) shows the Raman image constructed from the E_2 (high) phonon peak position of the GaN layer grown on GaN micro-pillar template fitted using a Lorentzian line shape from 560 cm^{-1} to 580 cm^{-1}. The Raman image clearly shows the hexagonal pattern with coalescing boundary and the coalescing point in bright yellow color, which arises from E_2 (high) phonon peak shift from 569.1 cm^{-1} to about 570.3 cm^{-1}. Also, the black

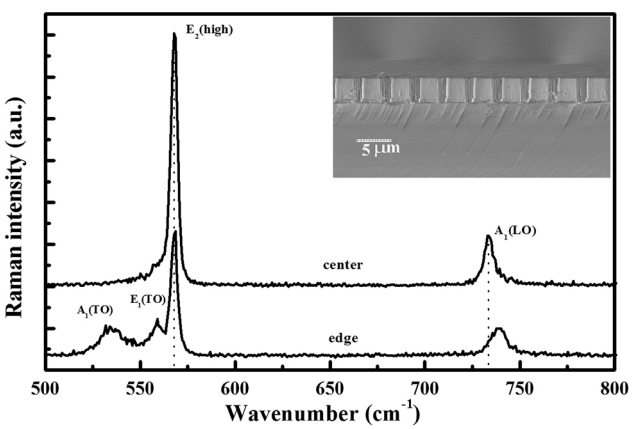

FIG. 1. Raman spectra of micro-pillar patterned GaN template measured in the center and the edge. The inset shows a SEM image of the micro-pillar patterned GaN template.

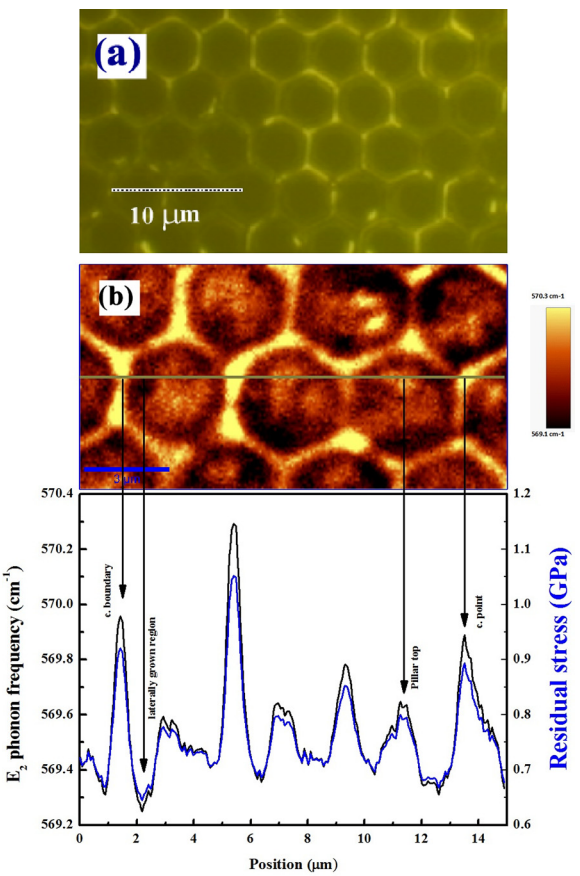

FIG. 2. (a) Optical microcopy image of completely coalesced smooth 5 μm thick GaN layer grown on micro-pillar GaN template. (b) Raman mapping of E_2 (high) phonon of a smooth 5 μm thick GaN layer grown on micro-pillar patterned GaN template measured in the region of 560 cm^{-1}–580 cm^{-1}. The scale bar shows the frequency position.

color regions are visible close to the coalescing boundary and point. This region grows laterally from the sidewall of the GaN micropillar template, and a line profile of E_2 (high) phonon peak position across the horizontal line is shown below. The line profile shows that (i) the entire E_2 (high) phonon is shifted to higher wavenumber compared to the strain-free thick GaN (567.6 cm^{-1}), it is also seen that the wavenumber is shifted, (ii) upwards in the coalescing boundary, and (iii) downwards in the laterally grown region. Maxima and minima of the E_2 (high) phonon frequency are observed at 570.3 cm^{-1} at the coalescing boundary and at 569.1 cm^{-1} at the laterally grown regions. The relation between E_2 (high) phonon frequency shift and the residual stress is given by[12] $\Delta\omega(cm^{-1}) = \omega - \omega_0 = K\Delta\sigma_{xx}$, where ω and ω_s are the E_2 (high) phonon frequencies of GaN on micro-pillar patterned GaN template and bulk GaN, respectively. K (cm^{-1}/GPa) is proportionality constant and equal to 2.56 cm^{-1}/GPa.[16] $\Delta\sigma_{xx}$ is the in-plane stress. The calculated residual stress value of the top surface of the GaN layer is shown in blue color in Figure 2(b). The maximum compressive stress is 1.05 GPa at the coalescing boundary and the minimum is 0.65 GPa at the laterally grown region. The stress is approximately 0.8 GPa at the top of the pillar region.

The maximum stress relaxation (minimum stress value) is observed in the laterally grown region, which is close to the coalescing boundary area. To further understand the stress relaxation in the laterally grown region, we have performed A_1(LO) phonon mapping. Figure 3 shows the Raman intensity image of A_1 (LO) phonon fitted using Gaussian line shape from 720 cm^{-1} to 760 cm^{-1}, and the corresponding peak position is shown. The mapping shows the sixfold symmetry (seen as black color) in the laterally grown region around the c-axis with {1–1 0 0} sidewalls, which is more clearly visible than in

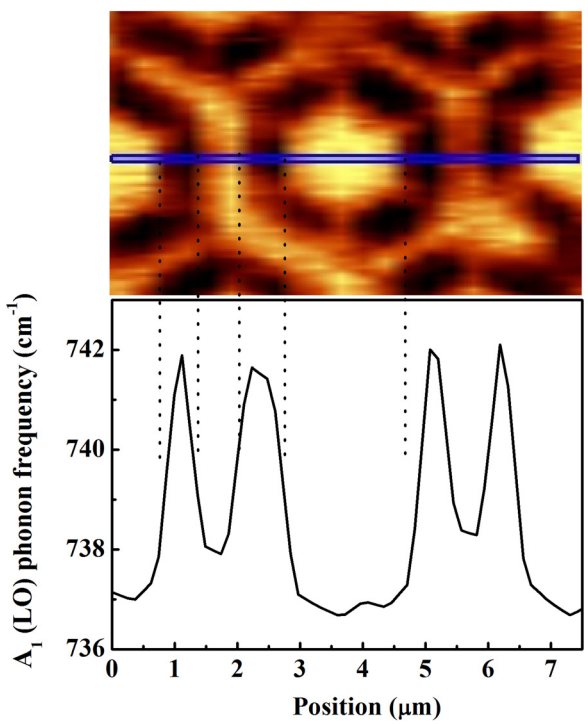

FIG. 3. Raman mapping of coalesced smooth 5 μm thick GaN layer grown on micro-pillar patterned GaN template measured in the region of 730 cm^{-1}–760 cm^{-1} (A_1(LO) phonon).

the E_2 (high) phonon (non-polar) mapping (Figure 2(b)). The A_1(LO) phonon frequency at the top surface of the pillar region is observed at 736.8 cm^{-1}. On the other hand, the A_1(LO) phonon frequency is observed at 742 cm^{-1} in the laterally grown region and at the coalescing boundary, the A_1(LO) phonon frequency is observed at about 737.8 cm^{-1}, which is located close to the A_1 (LO) phonon mode. Previously, the A_1(LO) phonon shift to higher frequency, due to phonon-plasmon coupled mode, has been studied in ELO GaN.[8] In this case, Si atom diffuse into the GaN layer from the SiO_2 stripes, which causes the relaxation of strain in the layer. However, in our case, the increase of A_1(LO) phonon from 736.8 cm^{-1} (top surface of pillar) to 742 cm^{-1} towards the center of the laterally grown region is observed due to the mixing of A_1(LO) phonon with E_1(LO) phonon. In our Raman experiments, we have used $z(x,x)\bar{z}$ backscattering configuration, which allows E_2 (high) and A_1(LO) phonon mode. However, E_1(LO) phonon is forbidden by the selection rule from the geometry used in our Raman measurements.[17] Previously, the mixing of A_1(LO) and E_1(LO) phonon mode has been reported as quasilongitudinal (QLO) modes due to the surface tilt relative to the c-axis in ELO GaN layer.[18] Based on our SEM image shown in Ref. 11, inclined {1 −1 0 1} growth facets are formed around the micro-pillars prior to film coalescence. The observation of QLO mode is related to the tilted facets around the micro-pillars. The tilted facets cause the light refraction away from the normal incidence. The intermediate energies of the QLO mode lie between the A_1(LO) and E_1(LO) phonon mode can be calculated using[19] $\omega^2_{QLO}(LO) = \omega^2_{A1(LO)}\cos^2(\theta) + \omega^2_{E1(LO)}\sin^2(\theta)$, where θ is the angle between phonon propagation direction and c-axis of the sample. The LO phonon has a frequency between that of the A_1(LO) mode (phonon propagation along the c-axis, θ is equal to 0°) and that of E_1(LO) phonon mode (θ is equal to 90°).[20] This indicates that phonon propagation is along the c-axis in the area on top of the pillar region meaning that this region has (0 0 0 1) c-axis. On the other hand, the observed A_1(LO) phonon frequency at 742 cm^{-1} in the laterally grown region is close to the E_1(LO) phonon mode of 743 cm^{-1}, which means that the phonon propagation is tilted from the c-axis.

This region is corresponding to the maximum stress relaxation (laterally grown region) observed in E_2 (high) phonon mapping. This indicates that the GaN grown from the {1–1 0 0} sidewall of the GaN micropillar, which does not have direct contact with the sapphire substrate causes the minimum stress value. A difference in compressive stress of 0.15 GPa between the top of the pillar region (vertical growth) and lateral growth is determined. We conclude that the stress relaxation in the laterally grown region is due to the GaN grown lateral direction from the sidewall of the GaN micropillar.

On the other hand, the maximum stress is observed in the coalescing boundary from the top surface of the GaN layer (Fig. 2(b)). Previously, increasing compressive stress in coalescing boundary compared to the wing region is reported in ELO GaN.[21] This compressive stress at coalescing boundary in ELO GaN has been attributed to (i) void formation and (ii) crystallographic tilting. The stress concentration with different void geometries in ELO GaN has been studied by finite element analysis and Raman measurement.[22] Also, it has

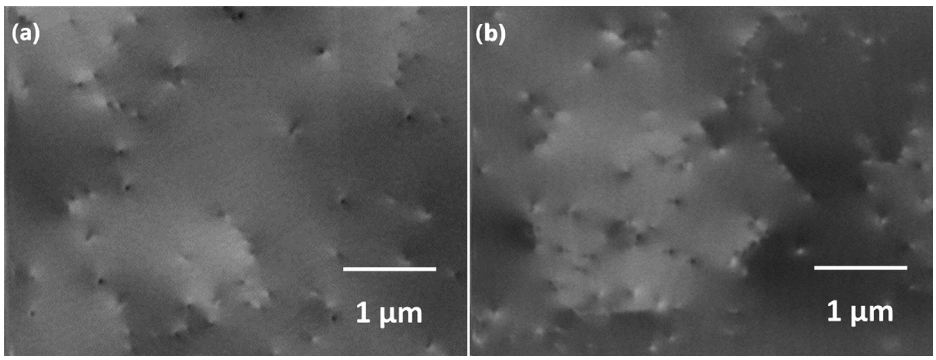

FIG. 4. ECC image of (a) GaN layer grown on GaN micro-pillar template and (b) 5-μm-thick GaN layer grown directly on sapphire substrate.

been suggested that a thick overgrowth of the GaN is necessary to reduce the effect of voids on stress at the surface of the GaN layer. On the other hand, the possible mechanism for a compressive stress at the coalescing boundary is crystallographic tilting. In the coalescence boundary, the crystallographic tilt originates from the self-organized propagation of dislocations coming from the micro-pillar region which bundle the dislocation along the void direction. This bundling effect helps to reduce the vertical dislocation density.[23]

To further understand the effect of dislocation formation on stress in the coalesced GaN over grown layer, we have performed electron channeling contrast imaging (ECCI) in a field emission scanning electron microscope. Changes in crystallographic orientation or changes in lattice constant due to local strain are revealed in ECCI as changes in grey scale in an image constructed by monitoring the intensity of backscattered electrons, when the electron beam is scanned over a suitably oriented sample. Extremely small orientation changes are detectable, enabling small angle tilt and rotation boundaries and dislocations to be imaged. Images with a resolution of tens of nanometers are obtainable in ECCI. More detailed information on ECCI is given elsewhere.[24] In ECCI, vertical TDs are revealed as spots with black-white (B-W) contrast. Figure 4 shows typical ECC images of the 5-μm-thick GaN layer grown on the micropillar patterned GaN template (a) and of a 5-μm-thick GaN layer grown on a sapphire substrate (b), revealing TDs and low angle grain boundaries. By counting the B-W spots, the dislocation density can be estimated. The TDs in the GaN grown on the micropillar patterned GaN template appear to be randomly distributed with no apparent correlation to the underlying template. The total TD density (edge, screw, and mixed) was estimated to be $1.5 \times 10^8\,\mathrm{cm}^{-2}$. This is lower than the dislocation density for the GaN layer grown directly on sapphire ($3.3 \times 10^8\,\mathrm{cm}^{-2}$). This illustrates that the use of a micropillar patterned GaN template is indeed useful for the reduction of the dislocation density in a subsequently overgrown layer.

In summary, we have performed Raman mapping of a GaN layer grown on micro-pillar patterned GaN template. Raman mapping of E_2 (high) phonon clearly reveals the stress distribution in different regions of the top surface of the pillar, the coalescing boundary and GaN grown in lateral direction. The maximum stress relaxation is observed in laterally grown GaN region close to the coalescing boundary. The A_1(LO) phonon shifts close to E_1(LO) phonon in between on top of the pillar region and the coalescing boundary, which is an evidence of GaN growth from the sidewall of the micro-pillar template. The maximum stress is observed in the coalescing boundary due to crystallographic tilting and voids.

This work was supported by the Academy of Finland through Project No. 13256332.

[1]Y. Li, S. You, M. Zhu, L. Zhao, W. Hou, T. Detchprohm, Y. Taniguchi, N. Tamura, S. Tanaka, and C. Wetzel, Appl. Phys. Lett. **98**, 151102 (2011).
[2]M. F. Schubert, S. Chhajed, J. K. Kim, and E. F. Schubert, Appl. Phys. Lett. **91**, 231114 (2007).
[3]T. Kozawa, T. Kachi, H. Kano, H. Nagase, N. Koide, and K. Manabe, J. Appl. Phys. **77**(9), 4389 (1995).
[4]D. Won, X. Weng, and J. M. Redwing, J. Appl. Phys. **108**, 093511 (2010).
[5]S. Dassonneville, A. Amokrane, B. Sieber, J.-L. Farvacque, B. Beaumont, and P. Gibart, J. Appl. Phys. **89**, 3736 (2001).
[6]T. S. Zheleva, S. A. Smith, D. B. Thomson, K. J. Linthicum, P. Rajagopal, and R. F. Davis, J. Electron. Mater. **28**, L5 (1999).
[7]E.-H. Park, J. Jang, S. Gupta, I. Ferguson, C.-H. Kim, S.-K. Jeon, and J.-S. Park, Appl. Phys. Lett. **93**, 191103 (2008).
[8]V. V. Chaldyshev, F. H. Pollak, M. Pophristic, S. P. Guo, and I. Ferguson, J. Appl. Phys. **92**, 6601 (2002).
[9]U. T. Schwarz, P. J. Schuck, M. D. Mason, R. D. Grober, A. M. Roskowski, S. Einfeldt, and R. F. Davis, Phys. Rev. B **67**, 045321 (2003).
[10]M. Ali, A. E. Romanov, S. Suihkonen, O. Svensk, P. T. Torma, M. Sopanen, H. Lipsanen, M. A. Odnoblyudov, and V. E. Bougrov, J. Cryst. Growth **315**, 188 (2011).
[11]O. Svensk, M. Ali, L. Riuttanen, P. T. Törmä, S. Sintonen, S. Suihkonen, M. Sopanen, and H. Lipsanen, J. Cryst. Growth **370**, 42 (2013).
[12]C. Kisielowski, J. Kruger, S. Ruvimov, T. Suski, J. W. Ager III, E. Jones, Z. Liliental-Weber, M. Rubin, and E. R. Weber, Phys. Rev. B **54**, 17745 (1996).
[13]V. Yu. Davydov, Yu. E. Kitaev, I. N. Goncharuk, A. N. Smirnov, J. Graul, O. Semchinova, D. Uffmann, M. B. Smirnov, A. P. Mirgorodsky, and R. A. Evarestov, Phys. Rev. B **58**, 12899 (1998).
[14]T. Azuhata, T. Sota, K. Suzuki, and S. Nakamura, J. Phys. Condens. Matter **7**, L129 (1995).
[15]O. Martinez, M. Avella, J. Jimenez, B. Gerard, R. Cusco, and L. Artus, J. Appl. Phys. **96**, 3639 (2004).
[16]J. W. Wagner and F. Bechstedt, Appl. Phys. Lett. **77**, 346 (2000).
[17]H. Harima, J. Phys: Condens. Matter. **14**, R967–R993 (2002).
[18]M. Benyoucef, M. Kuball, B. Beaumont, and P. Gibart, Appl. Phys. Lett. **80**, 2275 (2002).
[19]R. Loudan, Adv. Phys. **13**, 423 (1964).
[20]L. Shi, F. A. Ponce, and J. Menendez, Appl. Phys. Lett. **84**, 3471 (2004).
[21]M. Kuball, M. Benyoucef, B. Beaumont, and P. Gibart, J. Appl. Phys. **90**, 3656 (2001).
[22]M. Benyoucef, M. Kuball, G. Hill, M. Wisnom, B. Beaumont, and P. Gibart, Appl. Phys. Lett. **79**, 4127 (2001).
[23]A. Sakai, H. Sunakawa, A. Kimura, and A. Usui, Appl. Phys. Lett. **76**, 442 (2000).
[24]G. Naresh-kumar, B. Hourahine, P. R. Edwards, A. P. Day, A. Winkelmann, A. J. Wilkinson, P. J. Parbrook, G. England, and C. Trager-Cowan, Phys. Rev. Lett. **108**, 135503 (2012).